Peer-Reviewed Technical Communication

Sparse Direct Adaptive Equalization for Single-Carrier MIMO Underwater Acoustic Communications

Jun Tao, Yanbo Wu, Xiao Han, and Konstantinos Pelekanakis

***Abstract*—The sparse direct adaptive equalization technique recently received many attentions for single-carrier underwater acoustic communications. By taking advantage of the sparse (nonuniform) structure of a direct adaptive equalizer (DAE), one obtains a sparse DAE with improved performance and/or reduced complexity compared with its nonsparse counterpart. In this article, the sparse DAE is revisited with two contributions made: First, a comprehensive comparison is made for existing sparse DAEs designed with the proportionate-updating (PU) or the zero-attracting (ZA) adaptive filtering principles. The comparison concludes that the PU-type DAE outperforms the ZA-type DAE in terms of complexity, performance, and operability, thus shall be favored in practical use. Moreover, it motivates the design of a sparse DAE, named the selective ZA improved proportionate normalized least mean squares DAE (SZA-IPNLMS-DAE), based on the combination of the PU and ZA principles. The SZA-IPNLMS-DAE outperforms existing sparse DAEs armed with only one sparsity-promoting mechanism; second, a partial tap update (PTU) scheme via hard thresholding is introduced to sparse DAEs for reducing their complexity without sacrificing performance. The resulting low-complexity and high-performance sparse PTU-DAE schemes are strong candidates for single-carrier UWA communications. Experimental results of multiple-input multiple-output UWA communications are presented to corroborate all above claims.**

Manuscript received November 8, 2018; revised May 27, 2019; accepted October 3, 2019. Date of publication November 7, 2019; date of current version October 13, 2020. This work was supported in part by the National Natural Science Foundation of China under Grants 61871114, 61471351, and 11574048; in part by the Fund and Stable Supporting Fund of Acoustic Science and Technology Laboratory, Harbin Engineering University, under Grant SSJSWDZC2018013; in part by the Open Funds of State Key Laboratory of Acoustics, Chinese Academy of Sciences, under Grant SKLA201805; in part by the Six Talent Peaks Project in Jiangsu Province under Grant 2018-KTHY-001; in part by the Priority Academic Program Development of Jiangsu Higher Eduction Institutions under Grant 1104007112; in part by the Fund of Science and Technology on Sonar Laboratory under Grant 614210902111902; in part by the Natural Science Foundation of Jiangsu Province under Grant BK20160701; in part by the Fund for returning students to study abroad in Nanjing under Grant 1104000385; and in part by the Fundamental Research Fund of Southeast University under Grant 3204009407. *(Corresponding author: Jun Tao.)*

Associate Editor: J. Gomes.

J. Tao is with the Key Laboratory of Underwater Acoustic Signal Processing of the Ministry of Education, School of Information Science and Engineering, Southeast University, Nanjing 210096, China, with the Acoustic Science and Technology Laboratory, Harbin Engineering University, Harbin 150001, China, and also with the State Key Laboratory of Acoustics, Institute of Acoustics, Chinese Academy of Sciences, Beijing 100190, China (e-mail: jtao@seu.edu.cn).

Y. Wu is with the State Key Laboratory of Acoustics, Institute of Acoustics, Chinese Academy of Sciences, Beijing 100190, China, and also with the Beijing Engineering Technology Research Center of Ocean Acoustic Equipment, Beijing 100190, China (e-mail: wuyanbo@mail.ioa.ac.cn).

X. Han is with the Acoustic Science and Technology Laboratory, Harbin Engineering University, Harbin 150001, China (e-mail: hanxiao1322@hrbeu.edu.cn).

K. Pelekanakis is with the NATO Science and Technology Organization, Centre for Maritime Research and Experimentation, La Spezia 19126, Italy (e-mail: konstantinos.pelekanakis@cmre.nato.int).

Digital Object Identifier 10.1109/JOE.2019.2946679

***Index Terms*—Direct adaptive equalizer (DAE), multiple-input multiple-output (MIMO), sparse adaptive filtering, underwater acoustic (UWA) communications.**

I. Introduction

FOR single-carrier underwater acoustic (UWA) communications, there are two main types of equalizer design: the direct adaptive equalizer (DAE) [1], [2] and the channel-estimation-based equalizer (CEE) [3]–[5]. Due to the serious Doppler effect in an underwater channel, a complementary phase tracking and compensating module is usually required in both types for a good performance. As an example, a second-order phase-locked loop (PLL) has been adopted for the DAE in [1]. When the channel variation is slow, the CEE can be implemented in the frequency domain with robust performance and low complexity [4]. Under harsh channel conditions with extensive time dispersion and rapid variations, however, a CEE may suffer high complexity and/or significant degradation in both transmission efficiency and performance. The DAE, on the contrary, can achieve a good complexity-performance tradeoff, attributed to its symbol-wise equalization without explicit channel estimation. Overall, the DAE remains to be the most popular receiver technique for single-carrier UWA communications.

The DAE was initially implemented with the recursive least squares (RLS) adaptive algorithm [1] or the least mean squares (LMS) adaptive algorithm [2], and has been extensively developed ever since [6]–[13]. In [6], the RLS-DAE proposed in [1] for a multichannel transmission, or equivalently a single-input multiple-output transmission, was extended to the scenarios of multiple-input–multiple-output (MIMO) communications. Moreover, it was endowed the soft-input soft-output capability to enable the turbo equalization for improved performance. In [7], the RLS-DAE was implemented in the frequency domain, so as to reduce the equalization complexity. In [8], the LMS-DAE with a second-order PLL was tested by experimental data with high-order modulations of 16QAM and 32QAM. In [9], a fast self-optimized LMS (FOLMS) bidirectional decision-feedback (FB) adaptive equalizer was proposed. Experimental results verified the performance gain owing to the optimized step size and the bidirectional structure. In [10], a minimum symbol error rate DAE was proposed, claiming to outperform a conventional DAE designed with the minimum mean square error (MMSE) criteria. In [11], a normalized LMS (NLMS) DAE was proposed. Compared with the standard LMS algorithm, the NLMS mitigates the gradient noise amplification [14]. Moreover, its step size selection is independent of the input energy, which is desirable for a receiver without using an automatic gain control module. The data reuse (DR) technique [15], which repeats the symbol-wise coefficient adaptation over the same block multiple times to effectively prolonged the training procedure, was employed. To reduce the equalization complexity, the partial tap update (PTU) idea initiated in [2] was also

introduced to the NLMS-DAE. Different from the PTU conception in [16] where a full-tap filter has significant taps constantly adapted while trivial ones unchanged, the PTU in [2] discards insignificant taps and leads to a partial-tap DAE with unequally spaced coefficients. The determination of the surviving (partial) taps relied on the channel knowledge, which had to be estimated. In [12], a simple while effective hard thresholding (HT) based PTU mechanism was proposed, to enable a low-complexity FOLMS-DAE. Compared with [2] and [11], the HT-based PTU does not require explicit channel information thus is a favored choice for practical use. Specifically, it run a full-tap adaptive equalizer during the training stage and once the training procedure was completed, the surviving equalizer taps were identified via the HT. In the subsequent data symbol detection, a partial-tap DAE with reduced size was employed. Experimental results showed the HT-based PTU-DAE achieved considerable complexity reduction without sacrificing the performance much. To improve the identification of surviving taps, the authors further proposed a multiple threshold method in [13]. The feasibility of employing the PTU mechanism implies the sparsity of a DAE. It is noted, however, even a strictly sparse channel may not lead to a sparse equalizer, due to factors of finite-length constraint, design criteria, and so on. Moreover, even the sparsity of a UWA channel is not always guaranteed [17]. Therefore, the "sparsity" of an equalizer shall be interpreted in the wide sense that a relatively small number of taps account for a large percentage of energy [18]. To quantitatively, rather than just qualitatively, evaluate the level of sparsity for a system, the sparseness measure has been defined [19].

In light of the advancement in the sparse adaptive filtering theory [20]–[23], the sparsity has also been utilized for improving the DAE performance. Two fundamental principles have been employed to design the sparse adaptive filtering algorithms: the proportionate-updating (PU) principle which applies a larger step size for a larger tap, and the ZA principle which attracts small taps to zero. A well-known PU-type adaptive filtering algorithm is the improved proportionate normalized LMS (IPNLMS) algorithm [20], and the ZA-LMS [22] is a representative ZA-type algorithm. Sparse DAEs based on the PU-type and ZA-type adaptive algorithms are found in [24]–[27] and [28]–[30], respectively, and have manifested improved performance over that of conventional nonsparse DAEs. In [24], the IPNLMS algorithm and its extension, the improved proportionate affine projection algorithm (IPAPA) [21], were adopted to implement the DAE, which showed extra performance gain over the RLS and NLMS DAEs. Further comparison between the IPAPA-DAE and the RLS-DAE was found in [25] and again, the IPAPA-DAE outperformed the RLS-DAE [31]. In [26] and [27], the IPNLMS-DAE was applied to the multichannel transmission and the MIMO transmission, respectively. Once again, experimental results verified its superior performance over that of nonsparse DAEs [8]. In [28], a family of ZA-type RLS DAEs were proposed for general, group, or mixed sparse UWA channels. The sparse RLS-DAEs were verified by experimental data collected in shallow-water lake and sea UWA communication trials at a range of 1 and 30 km, respectively. They showed extra performance gain over a classical RLS-DAE, at the cost of increased complexity though. To reduce the complexity of the sparse RLS-DAE, fast implementations have been recently proposed [29]. In [30], a selective ZA NLMS-DAE (SZA-NLMS-DAE) was proposed for UWA communications. It outperformed the NLMS-DAE, especially when the training overhead is limited.

From above, the PU-type and ZA-type sparse DAEs provide extra performance gain over their nonsparse counterparts. Even though, there are two aspects about the sparse DAEs yet to be investigated: First, it is unclear which sparsity-promoting principle, the PU or the ZA, shall be preferred in practical UWA communications; second, a sparse DAE pays the cost of increased complexity for a better performance, compared with a nonsparse one. To reduce its complexity without sacrificing performance remains an open problem. In this article, the aforementioned two aspects are addressed for a MIMO UWA communication, considered as a promising way to meet the ever-increasing demand on the transmission rate [6]. Without loss of generality, the LMS-type sparse DAEs are investigated and a similar study can be performed for the RLS-type DAEs. To proceed, the IPNLMS-DAE and the SZA-NLMS-DAE are first compared in terms of principle, complexity, operability, and performance, so as to gain insights on the choice of the sparse DAE for practical UWA communications. Comparison results show the IPNLMS-DAE has lower complexity and better performance than the SZA-NLMS-DAE. Moreover, the IPNLMS-DAE is more user-friendly, since it has less adaptive parameters to be tuned. As a byproduct of the comparison, a sparsity-aware DAE designed by combining the PU and ZA principles was proposed. It showed the resulting SZA-IPNLMS-DAE outperformed both the IPNLMS-DAE and the SZA-NLMS-DAE, even though the performance margin over the IPNLMS-DAE is insignificant; second, the feasibility of PTU via HT [12] is explored for sparse DAEs. With a proper threshold setting, all investigated sparse DAEs enjoyed complexity reduction without obviously sacrificing the performance. Actually in some scenarios, slight performance gain is achieved attributed to the alleviation of noise enhancement and error propagation with reduced number of equalizer taps. Our findings have been extensively verified by experimental data collected in two independent at-sea UWA communication trails.

The rest of this article is organized as follows. In Section II, the system model is described. The sparse DAEs are revisited in Section III, and a comparison between the IPNLMS-DAE and the SZA-LMS-DAE is made in Section IV. Section V presents experimental results, demonstrating the performance comparison among different sparse DAEs and their PTU versions. Section VI concludes this article.

Notation: The superscripts, $(\cdot)^*$, $(\cdot)^t$, and $(\cdot)^h$ represent, respectively, the conjugate, the transpose, and the Hermitian. The $\mathcal{C}^{P\times Q}$ represents a complex space of dimension P by Q. For a vector $\mathbf{a}\in\mathcal{C}^{P\times 1}$, its l_r-norm ($r=1,2$) is defined as $\|\mathbf{a}\|_r=(\sum_{p=1}^{P}|[\mathbf{a}]_p|^r)^{1/r}$ with $[\mathbf{a}]_p$ denoting its pth element and $|\cdot|$ being the absolute value operation. The infinity norm of $\mathbf{a}$ is defined as $\|\mathbf{a}\|_\infty=\max(|[\mathbf{a}]_1|,\ldots,|[\mathbf{a}]_P|)$. The $\mathbf{I}_P$ represents a $P\times P$ identity matrix, and $\mathrm{Im}[x]$ denotes the imaginary part of a complex number x. The pth diagonal element of a square matrix $\mathbf{A}$ is denoted as $[\mathbf{A}]_{p,p}$.

II. System Model

A MIMO UWA communication system with N transducers on the transmitter side and M hydrophones on the receiver side, is considered. At the transmitter, space-time coding like the space-time trellis coding, the layered space-time coding, etc., can be employed to achieve spatial diversity and/or to increase the transmission rate [6]. At the receiver, motion-induced wideband Doppler effect is first estimated and compensated [32]. After the Doppler preprocessing, the received signal on the mth hydrophone at the time k can be expressed as

$$y_{m,k}=\sum_{n=1}^{N}\left\{e^{j\phi_{n,m,k}}\sum_{l=0}^{L}h_{n,m}(k,l)x_{n,k-l}\right\}+v_{m,k} \qquad (1)$$

where $x_{n,k-l}$ is the transmitted symbol by the nth transducer, $h_{n,m}(k,l)$ and $\phi_{n,m,k}$ are, respectively, the lth tap and the phase rotation of the (n,m)th time-varying subchannel between the nth transducer and the mth hydrophone, and $v_{m,k}$ is an additive noise on the mth hydrophone. The cause of phase rotation can be the residual Doppler shift after preprocessing or the Doppler spread incurred by, e.g., the water dynamics. It is noted treating the slow-varying tap coefficient $h_{n,m}(k,l)$ and the fast-changing phase jitter $\phi_{n,m,k}$ separately in (1), is a common practice for UWA channels [1].

To combat the phase rotation, the intersymbol interference, and the multiplexing interference, the following equalization model is adopted [6]:

$$\hat{x}_{n,k} = \sum_{m=1}^{M} e^{-j\theta_{n,m,k}} \mathbf{w}_{n,m,k}^h \mathbf{y}_{m,k} - \mathbf{f}_{n,k}^h \mathbf{d}_{n,k} \tag{2}$$

where $\hat{x}_{n,k}$ denotes the equalized symbol of the nth transducer at the time k, $\theta_{n,m,k}$ and $\mathbf{w}_{n,m,k} \in \mathcal{C}^{(K_1+K_2+1)\times 1}$ are the PLL output and the feedforward (FF) equalizer vector corresponding to the (n,m)th subchannel, and $\mathbf{y}_{m,k} = [y_{m,k+K_1}, \ldots, y_{m,k-K_2}]^t \in \mathcal{C}^{(K_1+K_2+1)\times 1}$ collects the received samples on the mth hydrophone over the time window $[k-K_2, k+K_1]$, $\mathbf{f}_{n,k} \in \mathcal{C}^{N(K_3+K_4+1)\times 1}$ is the FB equalizer vector corresponding to the decision-FB sequence, $\mathbf{d}_{n,k}$, defined as

$$\mathbf{d}_{n,k} = [\tilde{\mathbf{x}}_{k+K_3} \cdots \tilde{\mathbf{x}}_k \, \tilde{\mathbf{x}}_{k-1} \, \tilde{\mathbf{x}}_{k-K_4}]^t \tag{3}$$

with $\tilde{\mathbf{x}}_{k+q} \in \mathcal{C}^{N\times 1}$ given by

$$\tilde{\mathbf{x}}_{k+q} = \begin{cases} [\tilde{x}_{1,k+q}, \tilde{x}_{2,k+q}, \ldots, \tilde{x}_{N,k+q}]^t & q \neq 0 \\ [\tilde{x}_{1,k}, \ldots, \tilde{x}_{n-1,k}, 0, \tilde{x}_{n+1,k} \ldots, \tilde{x}_{N,k}]^t & q = 0. \end{cases} \tag{4}$$

The choice of the parameters $\{K_i\}_{i=1}^4$ depends on the type of equalizer employed. For example, when a conventional linear equalizer (LE) [33] is adopted, $K_1 > 0, K_2 > 0$ and it is unnecessary to designate K_3, K_4 as the decision vector $\mathbf{d}_{n,k}$ vanishes in this case. When a conventional decision-FB equalizer (DFE) with hard decision FB is adopted, $K_1 > 0$, $K_2 = 0$, $K_3 = 0$, $K_4 > 0$ is the proper choice. The decision-FB vector $\mathbf{d}_{n,k}$ now consists of hard decisions of the past symbols and the equalized on-time symbols. For a soft-input–soft-output equalizer employed in a turbo equalization, $K_1 > 0, K_2 > 0, K_3 > 0, K_4 > 0$ shall be picked and the $\mathbf{d}_{n,k}$ is made up of soft decisions of the past, on-time, and future interfering symbols [34].

Remark: as pointed out in [1], it may not be necessary to run separate phase tracking for each of the receive branches, if there is sufficient coherency among their phase rotations and the modulation level is low. In this case, the equalization model in (2) can be simplified as

$$\hat{x}_{n,k} = e^{-j\theta_{n,k}} \sum_{m=1}^{M} \mathbf{w}_{n,m,k}^h \mathbf{y}_{m,k} - \mathbf{f}_{n,k}^h \mathbf{d}_{n,k}. \tag{5}$$

Now, one phase sequence $\theta_{n,k}$, instead of M phase sequences $\{\theta_{n,m,k}\}_{m=1}^M$, is tracked and compensated for detecting the nth transmission stream.

To facilitate the discussion, one defines $\mathbf{w}_{n,k}, \mathbf{r}_{n,k} \in \mathcal{C}^{M(K_1+K_2+1)\times 1}$ in the following:

$$\mathbf{w}_{n,k} = [\mathbf{w}_{n,1,k}^h \, \mathbf{w}_{n,2,k}^h \cdots \mathbf{w}_{n,M,k}^h]^h \tag{6a}$$

$$\mathbf{r}_{n,k} = [e^{j\theta_{n,1,k}} \mathbf{y}_{1,k}^h \, e^{j\theta_{n,2,k}} \mathbf{y}_{2,k}^h \cdots e^{j\theta_{n,M,k}} \mathbf{y}_{M,k}^h]^h. \tag{6b}$$

Now, (2) can be expressed in a compact form as follows:

$$\hat{x}_{n,k} = \mathbf{w}_{n,k}^h \mathbf{r}_{n,k} - \mathbf{f}_{n,k}^h \mathbf{d}_{n,k}. \tag{7}$$

III. Sparse Direct Adaptive Equalization

First, the phase tracking is briefly discussed. The instantaneous symbol estimation error is

$$e_{n,k} = x_{n,k} - \hat{x}_{n,k}. \tag{8}$$

Take the first derivative of the squared error, $J_{n,k} = |e_{n,k}|^2$, with respect to $\theta_{n,m,k}$, leading to

$$\frac{\partial J_{n,k}}{\partial \theta_{n,m,k}} = -2\mathrm{Im}[\hat{x}_{n,k}^m (\hat{x}_{n,k}^m + e_{n,k})^*] \tag{9}$$

where $\hat{x}_{n,k}^m = \mathbf{w}_{n,m,k}^h \mathbf{y}_{m,k} e^{-j\theta_{n,m,k}}$. Define

$$\Phi_{n,m,k} = \mathrm{Im}[\hat{x}_{n,k}^m (\hat{x}_{n,k}^m + e_{n,k})^*] \tag{10}$$

then the phase tracking via a second-order PLL is [1]

$$\theta_{n,m,k+1} = \theta_{n,m,k} + K_{f1}\Phi_{n,m,k} + K_{f2} \sum_{q=0}^{k} \Phi_{n,m,q} \tag{11}$$

with K_{f1} and K_{f2} being the PLL parameters.

Next, the tracking of the equalizer vectors via sparse adaptive filtering algorithms is discussed. Two sparse DAEs, the IPNLMS-DAE and the SZA-NLMS-DAE, are revisited in Section III-A and III-B.

A. IPNLMS-DAE

The IPNLMS-DAE has its equalizer vectors updated as [24]

$$\mathbf{w}_{n,k+1} = \mathbf{w}_{n,k} + \mu_w \frac{e_{n,k}^* \mathbf{G}_{n,k}^w \mathbf{r}_{n,k}}{\mathbf{r}_{n,k}^h \mathbf{G}_{n,k}^w \mathbf{r}_{n,k} + \delta_w} \tag{12a}$$

$$\mathbf{f}_{n,k+1} = \mathbf{f}_{n,k} - \mu_f \frac{e_{n,k}^* \mathbf{G}_{n,k}^f \mathbf{d}_{n,k}}{\mathbf{d}_{n,k}^h \mathbf{G}_{n,k}^f \mathbf{d}_{n,k} + \delta_f} \tag{12b}$$

where $e_{n,k}$ has been defined in (8), and $\mathbf{G}_{n,k}^w$ and $\mathbf{G}_{n,k}^f$ are diagonal matrices with their pth diagonal elements being

$$[\mathbf{G}_{n,k}^w]_{p,p} = \frac{1-\alpha}{2L_w} + (1+\alpha)\frac{|[\mathbf{w}_{n,k}]_p|}{2\|\mathbf{w}_{n,k}\|_1 + \epsilon_w} \tag{13a}$$

$$[\mathbf{G}_{n,k}^f]_{p,p} = \frac{1-\alpha}{2L_f} + (1+\alpha)\frac{|[\mathbf{f}_{n,k}]_p|}{2\|\mathbf{f}_{n,k}\|_1 + \epsilon_f} \tag{13b}$$

and $-1 \leq \alpha < 1$. The $L_w = M(K_1+K_2+1)$ and $L_f = N(K_3+K_4+1)$ are the sizes of the FF equalizer vector and the FB equalizer vector, respectively, and $\{\delta_w, \delta_f, \epsilon_w, \epsilon_f\}$ are small positive numbers introduced to avoid possible numerical issues during the equalization process. When $\alpha = -1$, the IPNLMS-DAE reduces to the conventional NLMS-DAE.

B. SZA-NLMS-DAE

To design the SZA-NLMS-DAE, l_1-norm penalty is introduced to the squared error $J_{n,k}$, leading to the regularized cost function as

$$\tilde{J}_{n,k} = |e_{n,k}|^2 + 2\gamma_w \|\mathbf{w}_{n,k}\|_1 + 2\gamma_f \|\mathbf{f}_{n,k}\|_1 \tag{14}$$

based on which the updating equations for the equalizer vectors are designed as [30]

$$\mathbf{w}_{n,k+1} = \mathbf{w}_{n,k} + \rho_w \frac{e_{n,k}^* \mathbf{r}_{n,k}}{\|\mathbf{r}_{n,k}\|_2^2 + \Delta_w} - \mathbf{Q}_{n,k}^w \bar{\mathbf{w}}_{n,k} \tag{15a}$$

$$\mathbf{f}_{n,k+1} = \mathbf{f}_{n,k} - \rho_f \frac{e_{n,k}^* \mathbf{d}_{n,k}}{\|\mathbf{d}_{n,k}\|_2^2 + \Delta_f} - \mathbf{Q}_{n,k}^f \bar{\mathbf{f}}_{n,k} \tag{15b}$$

where $\mathbf{Q}_{n,k}^w$ and $\mathbf{Q}_{n,k}^f$ are diagonal matrices with their pth diagonal elements being

$$[\mathbf{Q}_{n,k}^w]_{p,p} = \begin{cases} \gamma_w (1 - \frac{|[\mathbf{w}_{n,k}]_p|}{\beta_w \|\mathbf{w}_{n,k}\|_\infty}), & \frac{|[\mathbf{w}_{n,k}]_p|}{\|\mathbf{w}_{n,k}\|_\infty} < \beta_w \\ 0, & \frac{|[\mathbf{w}_{n,k}]_p|}{\|\mathbf{w}_{n,k}\|_\infty} \geq \beta_w \end{cases} \tag{16a}$$

$$[\mathbf{Q}_{n,k}^f]_{p,p} = \begin{cases} \gamma_f (1 - \frac{|[\mathbf{f}_{n,k}]_p|}{\beta_f \|\mathbf{f}_{n,k}\|_\infty}), & \frac{|[\mathbf{f}_{n,k}]_p|}{\|\mathbf{f}_{n,k}\|_\infty} < \beta_f \\ 0, & \frac{|[\mathbf{f}_{n,k}]_p|}{\|\mathbf{f}_{n,k}\|_\infty} \geq \beta_f. \end{cases} \tag{16b}$$

TABLE I
COMPARISON OF UPDATING TERMS BETWEEN THE IPNLMS-DAE AND THE SZA-NLMS-DAE

DAE / Term	IPNLMS	SZA-NLMS
1	$\mu'_w \frac{e^*_{n,k}\mathbf{r}_{n,k}}{\mathbf{r}^h_{n,k}\mathbf{G}^w_{n,k}\mathbf{r}_{n,k}+\delta_w}$	$\rho_w \frac{e^*_{n,k}\mathbf{r}_{n,k}}{\|\mathbf{r}_{n,k}\|_2^2+\Delta_w}$
2	$\mu_w \frac{e^*_{n,k}\mathbf{G}^{w,2}_{n,k}\mathbf{r}_{n,k}}{\mathbf{r}^h_{n,k}\mathbf{G}^w_{n,k}\mathbf{r}_{n,k}+\delta_w}$	$-\mathbf{Q}^w_{n,k}\bar{\mathbf{w}}_{n,k}$

The design of $\mathbf{Q}^w_{n,k}$ and $\mathbf{Q}^f_{n,k}$ in (16) has been motivated by [23]. Different from [23], however, normalization by $\|\mathbf{w}_{n,k}\|_\infty$ or $\|\mathbf{f}_{n,k}\|_\infty$ has been included to account for the unknown coefficient scaling in a practical system. The subgradient vector $\bar{\mathbf{w}}_{n,k}$ is defined as

$$\bar{\mathbf{w}}_{n,k} = \frac{\partial\|\mathbf{w}_{n,k}\|_1}{\partial\mathbf{w}^*_{n,k}} \tag{17}$$

with its evaluation referred to Appendix A, where the derivation of $(\partial\|\mathbf{a}\|_1/\partial\mathbf{a}^*)$ for a general vector $\mathbf{a}$ is detailed. From the results therein, the pth element of $\bar{\mathbf{w}}_{n,k}$ is obtained as

$$[\bar{\mathbf{w}}_{n,k}]_p = \begin{cases} \frac{[\mathbf{w}_{n,k}]_p}{|[\mathbf{w}_{n,k}]_p|}, & [\mathbf{w}_{n,k}]_p \neq 0 \\ 0, & [\mathbf{w}_{n,k}]_p = 0. \end{cases} \tag{18}$$

The subgradient vector $\bar{\mathbf{f}}_{n,k}$ can be similarly obtained and is not listed for brevity. Last, it is noted when $\gamma_w = \gamma_f = 0$ in (16), the SZA-NLMS-DAE reduces to the NLMS-DAE.

IV. COMPARISON BETWEEN THE IPNLMS-DAE AND THE SZA-NLMS-DAE

In this section, comparisons are made between the IPNLMS-DAE and the SZA-NLMS-DAE in terms of principle, complexity, and operability. For brevity, all comparisons are performed with the FF equalizer vectors and the results also apply to the FB equalizer vectors.

A. Principle Comparison

The $\mathbf{G}^w_{n,k}$ in (12a) is decomposed as

$$\mathbf{G}^w_{n,k} = \mathbf{G}^{w,1}_{n,k} + \mathbf{G}^{w,2}_{n,k} \tag{19}$$

where $\mathbf{G}^{w,1}_{n,k} = (1-\alpha)/(2L_w)\mathbf{I}_{L_w}$ is a scaled identity matrix and $\mathbf{G}^{w,2}_{n,k}$ is a diagonal matrix with its pth diagonal element being

$$\frac{(1+\alpha)|[\mathbf{w}_{n,k}]_p|}{2\|\mathbf{w}_{n,k}\|_1+\epsilon_w}.$$

Plugging (19) into (12a) leads to

$$\mathbf{w}_{n,k+1} = \mathbf{w}_{n,k} + \mu'_w \frac{e^*_{n,k}\mathbf{r}_{n,k}}{\mathbf{r}^h_{n,k}\mathbf{G}^w_{n,k}\mathbf{r}_{n,k}+\delta_w} + \mu_w \frac{e^*_{n,k}\mathbf{G}^{w,2}_{n,k}\mathbf{r}_{n,k}}{\mathbf{r}^h_{n,k}\mathbf{G}^w_{n,k}\mathbf{r}_{n,k}+\delta_w} \tag{20}$$

with $\mu'_w = (1-\alpha)/(2L_w)\mu_w$. From (20) and (15a), both equations have two updating terms, listed in Table I. The first updating terms for the two sparse DAEs share the same updating direction $e^*_{n,k}\mathbf{r}_{n,k}$, which is actually the descent direction of the standard LMS-DAE [2]. For convenience, it is called the "standard updating term." The second updating term of the IPNLMS-DAE has an updating direction $e^*_{n,k}\mathbf{G}^{w,2}_{n,k}\mathbf{r}_{n,k}$, which in effect employs a larger step size for a larger coefficient. For the SZA-NLMS-DAE, its second updating term has an updating direction of $-\mathbf{Q}^w_{n,k}\bar{\mathbf{w}}_{n,k}$, which attracts small coefficients [below some threshold as in (16a)] to zero. Both second updating terms account for the sparsity (nonuniformity) of the equalizer, thus are named the "sparsity-aware updating term." In general, the directions of the two sparsity-aware updating terms are different, so are the PU principle and the ZA principle. As a result, the PU and ZA principles can be combined, leading to a new sparse DAE with the following updating equation:

$$\mathbf{w}_{n,k+1} = \mathbf{w}_{n,k} + \mu_w \frac{e^*_{n,k}\mathbf{G}^w_{n,k}\mathbf{r}_{n,k}}{\mathbf{r}^h_{n,k}\mathbf{G}^w_{n,k}\mathbf{r}_{n,k}+\delta_w} - \mathbf{Q}^w_{n,k}\bar{\mathbf{w}}_{n,k}. \tag{21}$$

It is noted the sparse adaptive filtering algorithm combining the PU and ZA principles has been previously proposed in [25] for sparse channel estimation. Even though, it has not been applied in the channel equalization, to the best of our knowledge. For convenience, the sparse DAE designated by (21) is named the SZA-IPNLMS-DAE. It offers extra performance gain over either the IPNLMS-DAE or the SZA-NLMS-DAE, as will be shown in Section V.

B. Complexity Comparison

To facilitate the complexity comparison, the two sparsity-aware DAEs are compared with the standard NLMS-DAE. For the IPNLMS-DAE, the extra complexity over the NLMS-DAE lies in the computation of $\mathbf{G}^w_{n,k}$, $\mathbf{G}^w_{n,k}\mathbf{r}_{n,k}$, and $\mathbf{r}^h_{n,k}\mathbf{G}^w_{n,k}\mathbf{r}_{n,k}$. From (13a), the calculation of $\mathbf{G}^w_{n,k}$ involves the l_1-norm evaluation for $\mathbf{w}_{n,k}$, L_w real divisions (RDs), and L_w real multiplications (RMs) for each updating. The $(1-\alpha)/(2L_w)$ is a constant and its computation is ignored. The calculation of $\mathbf{G}^w_{n,k}\mathbf{r}_{n,k}$ incurs $2L_w$ RMs, and the $\mathbf{r}^h_{n,k}\mathbf{G}^w_{n,k}\mathbf{r}_{n,k}$ evaluation requires L_w RMs (noticing $\mathbf{r}^h_{n,k}\mathbf{r}_{n,k}$ is also needed for the NLMS-DAE). In summary, the IPNLMS-DAE requires an extra complexity of a size-L_w l_1-norm evaluation, $4L_w$ RMs, and L_w RDs for each updating, compared with the NLMS-DAE.

For the SZA-NLMS-DAE, the extra complexity over the NLMS-DAE lies in the computation of $\mathbf{Q}^w_{n,k}\bar{\mathbf{w}}_{n,k}$. For each updating, the extra computation involves an l_1-norm evaluation of $\mathbf{w}_{n,k}$ [as it requires the absolute value of each element in $\mathbf{w}_{n,k}$ from (16a) and (18)], $3L_w$ RDs, L_w comparison operations, $< 4L_w$ RMs [the exact number depends on the comparison results in (16a)], and one size-L_w infinity norm evaluation. Therefore, the SZA-NLMS-DAE has a higher complexity than the IPNLMS-DAE, as it demands more division operations. The complexity of the SZA-NLMS-DAE can be reduced by employing a simplified selection matrix with

$$[\mathbf{Q}^w_{n,k}]_{p,p} = \gamma_w, \qquad \text{for } \frac{|[\mathbf{w}_{n,k}]_p|}{\|\mathbf{w}_{n,k}\|_\infty} < \beta_w.$$

Despite the comparison, both sparse DAEs pay the cost of increased complexity for achieving extra performance gain. To reduce the complexity, the PTU strategy can be employed. The HT-based PTU scheme [12] is adopted herein. During the training stage, the full-tap FF and FB equalizer vectors with length L_w and L_f are used and once the training is complete, small taps below some threshold are discarded and new FF and FB equalizer vectors with reduced sizes, $L'_w < L_w$ and $L'_f < L_f$, are employed. The complexity ratio between the resulting partial-tap DAE and the original full-tap DAE is then

$$\gamma = \frac{(L_w+L_f)K_p + (L'_w+L'_f)K_d}{(L_w+L_f)K} \tag{22}$$

where K_p and K_d are the lengths of the training block and the data block, respectively, and $K = K_p + K_d$ is the size of an entire transmission block. It should be pointed out that a reduction in complexity does not always mean a degradation in performance. For example, running less number of FF taps helps to alleviate the noise enhancement issue [33]. Also, a reduced-size FB equalizer has a smaller chance of error propagation. If the gain brought by running a reduced-size DAE is more than enough to compensate the loss by discarding some contributing equalizer taps, a performance improvement will happen, as observed from the experimental results.

C. Operability Comparison

For the IPNLMS-DAE, proper choices of μ_w, μ_f, and α are important to its performance. The $\delta_w, \delta_f, \epsilon_w, \epsilon_f$ are introduced for avoiding numerical issues at initial stage, thus only have a small impact on the performance. From [20], good choices for α are 0 or -0.5 and our choice of $\alpha = 0$ for processing experimental data led to consistently satisfactory results. The selection of μ_w and μ_f obeys $0 < \mu_w, \mu_f < 2$ [14], [20], which is independent of the energy of the regression input.

As to the SZA-NLMS-DAE, key parameters for the performance include $\rho_w, \rho_f, \gamma_w, \gamma_f, \beta_w$, and β_f, and the Δ_w and Δ_f are trivial ones for avoiding numerical issues. The choice of ρ_w and ρ_f is similar to the selection of μ_w and μ_f for the IPNLMS-DAE. To find optimal γ_w and γ_f, an analytical study was performed in [22] and it showed both depend on the input energy. The analytical results rely on several assumptions though and for practical use, heuristic method is instead preferred [22], [23]. As to β_w and β_f, it is very difficult, if not impossible, to have an analytically optimal solution. Therefore, heuristic choices are required.

From above, the IPNLMS-DAE involves three key parameters whose determinations are relatively easy. On the contrary, the SZA-NLMS-DAE has six critical parameters to be decided. Some of them are input-dependent thus have to be chosen empirically. In summary, the IPNLMS-DAE is more user-friendly than the SZA-NLMS-DAE.

Last, the performance comparison is made. Analytical performance investigation for sparse adaptive filtering algorithms have been extensively studied in the literature [14], [19], [22], where assumptions and approximations are generally involved to make the problem tractable. For the system model of UWA channel equalization, the input samples to the equalizer are correlated and the additive noise is generally non-Gaussian, making those assumptions invalid. As a result, large discrepancy between analytical and actual performance may happen. Therefore, we resort to experimental results for the performance comparison among the sparse DAEs, as detailed in Section V.

V. Experimental Results

Experimental results of two at-sea UWA communication trials are presented in this section.

A. First Experiment

The first experiment was conducted off the coastline of New Jersey in 2009. On the transmitter side, the transducer array consisted of four elements, enabling a MIMO configuration with N up to 4. Two receive hydrophone arrays each with eight elements were deployed, with their distances to the transmitter being 2 and 3 km, respectively. The carrier frequency was 17 kHz and the symbol period was $T_s = 0.2$ ms. A rate-$(1/2)$ LDPC channel code was adopted. A single transmission burst consisted of 50 blocks each carrying $K = 1024$ symbols, for which the first K_p ones are used for training purpose. The multipath

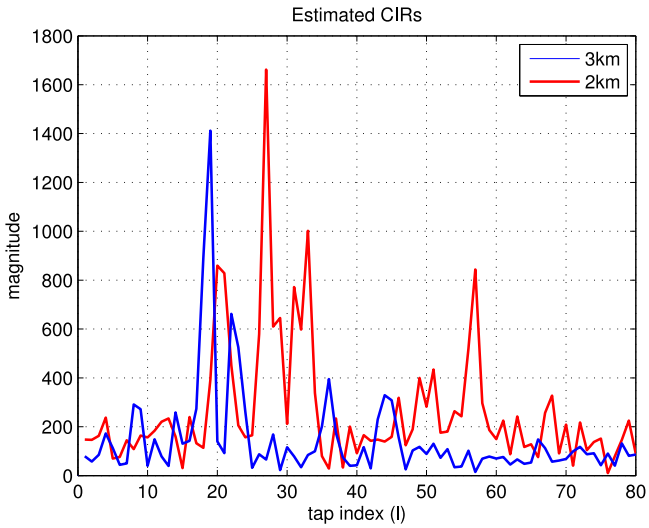

Fig. 1. Estimated CIRs for the first experiment.

spread of the channel was generally less than 80 in terms of symbol periods, as shown by the examples in Fig. 1. The simplified equalization model in (5) was adopted and a conventional DFE with hard decision FB was employed. The sizes of the FF and FB equalizer vectors are 40 per receive channel and 50 per transmit stream, respectively. Therefore, $K_1 = 40$, $K_2 = 0$, $K_3 = -1$ (the on-time decision FB is ignored), and $K_4 = 50$. For an $N \times M$ MIMO transmission, $L_w = 41\,M$ and $L_f = 50\,N$.

The experimental results for a 1×8 multichannel transmission with 16QAM modulation and $K_p = 250$ are first presented. As $N = 1$ and $M = 8$, the sizes of the FF equalizer vector, $\mathbf{w}_{n,k}$, and the FB equalizer vector, $\mathbf{f}_{n,k}$, were $L_w = 328$ and $L_f = 50$, respectively. The adaptive parameters for the SZA-NLMS-DAE were: $\rho_w = \rho_f = 0.2$, $\Delta_w = \Delta_f = 1$, $\beta_w = 0.05$, $\beta_f = 0.1$, $\gamma_w = 6.0 \times 10^{-9}$, and $\gamma_f = 1.3 \times 10^{-4}$. It is noted such choices of γ_w and γ_f were based on the rule of thumb that they are 10^{-4} of the median of the filter tap magnitude [22], [23]. Based on the SZA-NLMS-DAE, the NLMS-DAE was obtained by setting $\gamma_w = \gamma_f = 0$ as already mentioned. The adaptive parameters for the IPNLMS-DAE were: $\mu_w = \mu_f = 0.2$, $\delta_w = \delta_f = 1$, $\alpha = 0$ and $\epsilon_w = \epsilon_f = 10^{-9}$. Based on the IPNLMS-DAE, an SZA term with parameters $\beta_w = 0.05$, $\beta_f = 0.1$, $\gamma_w = 1.2 \times 10^{-10}$, and $\gamma_f = 1.07 \times 10^{-5}$ were introduced to implement the SZA-IPNLMS-DAE. Compared with the SZA-NLMS-DAE, smaller values of γ_w and γ_f were adopted for compromising the PU mechanism. The HT thresholds (0.01,0.01) were adopted for the FF and FB equalizer vectors, to achieve the PTU DAEs. A threshold of 0.01 means taps of magnitude less than 1% of the maximum magnitude will be discarded once the training is completed, and such a choice is conservative. For all investigated DAEs, the same PLL parameters $K_{f1} = 0.0067$ and $K_{f2} = K_{f1}/10$ were used.

At each transmission range, five bursts were recorded and processed. The average SNRs were 14.5 and 12.7 dB for the 3- and 2-km transmission, respectively. The number of error-free blocks (NEFB) after channel decoding for ten detected bursts (500 blocks) are listed in Table II, where N_{dr} denotes the DR repeat times. It is noted for a given DR repeat number N_{dr}, the actual number of passes through the training block will be $N_{\text{dr}} + 1$. The same results are also compared via bar graph in Fig. 2 for a better illustration. From the results, several

TABLE II
NEFB COMPARISON (1×8, 16QAM, 500 BLOCKS IN TOTAL)

DAE \ N_{dr}	2	4	6
NLMS	35	142	223
PTU-NLMS	35	151	225
IPNLMS	250	363	397
PTU-IPNLMS	276	368	400
SZA-NLMS	79	229	289
PTU-SZA-NLMS	58	201	284
SZA-IPNLMS	277	372	414
PTU-SZA-IPNLMS	270	367	405

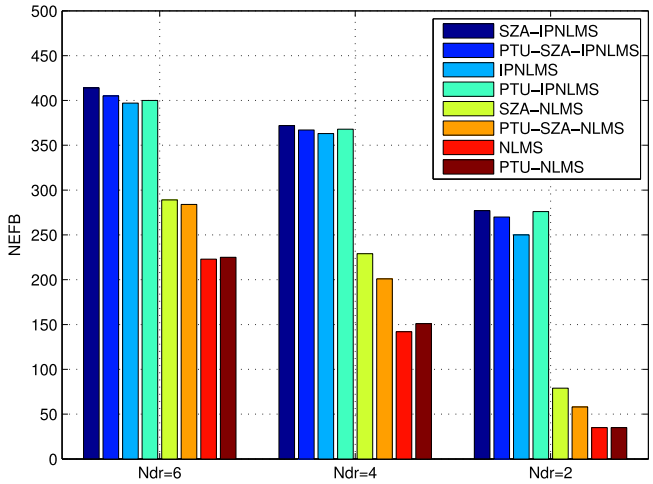

Fig. 2. Comparison of the NEFB (1×8, 16QAM, 500 blocks in total).

TABLE III
COMPLEXITY PERCENTAGE OF THE PTU-DAE TO THE FULL-TAP DAE (1×8, 16QAM)

DAE \ N_{dr}	2	4	6
PTU-NLMS	95.71%	95.71%	95.96%
PTU-IPNLMS	60.52%	64.16%	66.31%
PTU-SZA-NLMS	72.61%	61.33%	55.68%
PTU-SZA-IPNLMS	58.08%	60.49%	61.79%

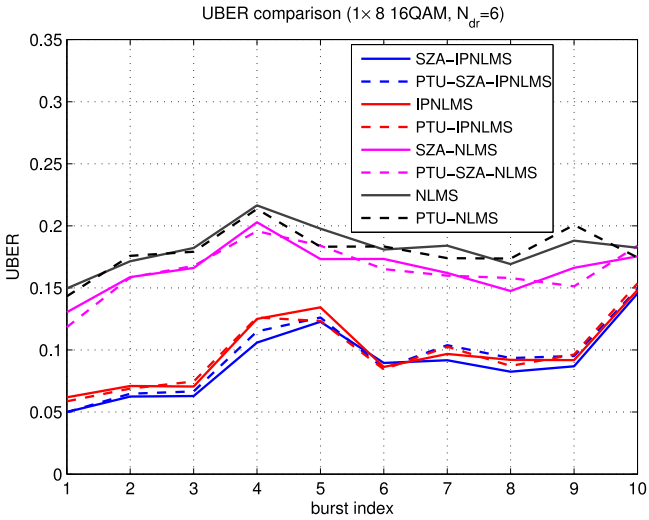

Fig. 3. Comparison of the uncoded BER (1×8, 16QAM).

observations are made: First, all sparse DAEs outperform the non-sparse NLMS-DAE, as expected; second, the SZA-IPNLMS-DAE and IPNLMS-DAE both considerably outperform the SZA-NLMS-DAE, and the SZA-IPNLMS-DAE slightly outperforms the IPNLMS-DAE. This observation indicates the PU principle is a better choice than the ZA principle for the DAE application; last, for each DAE, its PTU version achieves a comparable performance. For the NLMS-DAE and IPNLMS-DAE, their PTU versions actually provide extra performance gain, due to the conservative choices of HT thresholds and the reason explained at the end of Section IV-B. For the SZA-NLMS-DAE and SZA-IPNLMS-DAE, on the contrary, the PTU versions suffer slight performance degradation. The reason is that with the ZA principle, small taps are attracted to zeros and the HT operation has a higher chance to drop contributing taps.

The complexity percentage of the PTU DAEs to their full-tap counterparts are listed in Table III. From the table, the PTU-NLMS-DAE only has a slight complexity reduction (less than 5%). For the sparsity-aware DAEs, however, considerable complexity savings are achieved. Take $N_{\rm dr} = 6$ as an example, the PTU-SZA-NLMS-DAE saves about 45% computation. The saving percentages for the PTU-SZA-IPNLMS-DAE and the PTU-IPNLMS-DAE are close to 40% and 35%, respectively. This observation indicates the sparsity-aware DAEs not only improve the performance but also promotes the complexity reduction (through the PTU scheme), compared with nonsparse DAEs. Last, it shall be mentioned that for a given DAE, the complexity saving depends on the DR number $N_{\rm dr}$. The reason is that different $N_{\rm dr}$ leads to generally different DAE tap profile at the end of training stage, thus different number of surviving taps.

The uncoded bit error rate (UBER) as a complementary performance metric to the NEFB are compared in Fig. 3, where the results with $N_{\rm dr} = 6$ are shown. In general, the UBER comparison is consistent with the NEFB comparison. It is noted the UBER performance can be further improved by adopting the equalization model (2), where each receive branch runs an individual PLL.

In Fig. 4, the FF equalizer vectors at the end of one processed block are depicted for the four PTU-DAEs, where an increased HT threshold 0.02 has been used for a better demonstration. The discarded taps are shown as zeros in the figures. Obviously, the PTU-SZA-IPNLMS-DAE and PTU-IPNLMS-DAE only keep less than 50% surviving taps while the PTU-NLMS-DAE has almost all taps survived. The number of survival taps for the PTU-SZA-NMLS-DAE is between those of the PTU-NLMS-DAE and PTU-SZA-IPNLMS-DAE (or PTU-IPNLMS-DAE).

Next, the results for a 2×4 QPSK transmission with $K_p = 200$ are presented. As $N = 2$ and $M = 4$, the sizes of the FF equalizer vector and the FB equalizer vector were $L_w = 164$ and $L_f = 100$, respectively. The DAE parameters were the same as those adopted in the 1×8 16QAM transmission. Two sets of HT thresholds (0.01,0.01) (I) and (0.05,0.05) (II) were considered when implementing the PTU DAEs. The comparisons based on five detected bursts (250 blocks) of 3 km transmission are shown in Table IV. In general, the comparison is similar to that of the 1×8 16QAM transmission. The HT threshold

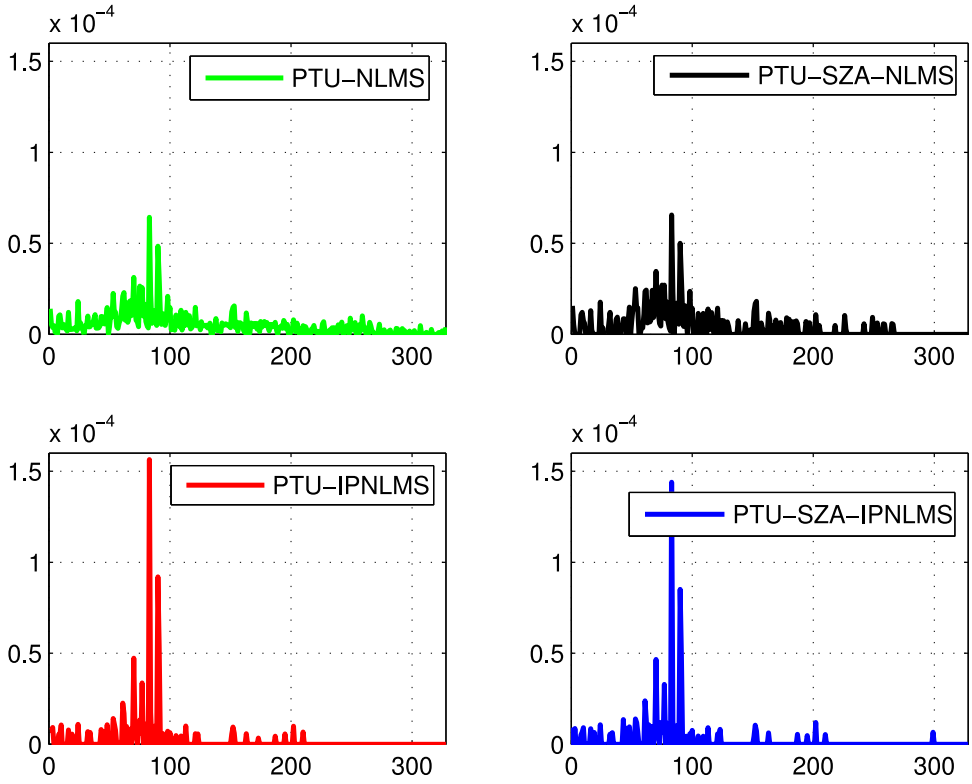

Fig. 4. Comparison of the converged FF equalizer coefficients among the PTU-DAEs.

TABLE IV
NEFB COMPARISON (2×4, QPSK, 250 BLOCKS IN TOTAL)

DAE \ N_{dr}	2	4	6
NLMS	0	11	25
PTU-NLMS(I)	0	9	23
PTU-NLMS(II)	0	12	25
IPNLMS	203	220	222
PTU-IPNLMS(I)	204	221	221
PTU-IPNLMS(II)	161	200	214
SZA-NLMS	7	42	81
PTU-SZA-NLMS(I)	0	39	79
PTU-SZA-NLMS(II)	4	55	84
SZA-IPNLMS	210	224	225
PTU-SZA-IPNLMS(I)	207	223	226
PTU-SZA-IPNLMS(II)	164	206	214
RLS	233	229	228
SFTF	203	223	224

has visible impact on the performance: for the PTU-SZA-IPNLMS-DAE and PTU-IPNLMS-DAE, moderate performance degradation is observed when the threshold increases from 0.01 to 0.05. The PTU-NLMS-DAE and PTU-SZA-NLMS-DAE nevertheless achieve slight performance gain. The result of the RLS-DAE with a forgetting factor $\lambda = 0.999$, is also included in Table IV. At $N_{\text{dr}} = 2$, the RLS-DAE outperforms all LMS-type DAEs attributed to its fast convergence. Actually, at $N_{\text{dr}} = 0$ (not shown), the RLS-DAE already achieves the same NEFB as that of $N_{\text{dr}} = 2$. The use of DR does not affect the RLS-DAE performance much. The reason is that the DR does not change the LS equation set and its impact is exerted mainly on the initialization. The standard RLS has an impractically high complexity and its fast implementation via the stable fast transversal filter (SFTF) algorithm [35] was also tested. Compared with the RLS-DAE, the SFTF-DAE suffers some performance degradation. However, it benefits from the DR and achieves comparable performance to that of the IPNLMS-DAE. The reason is that compared with the RLS, the SFTF involves additional parameters (some are heuristically chosen [35]), causing performance loss which nevertheless is compensated by the DR. Despite its decent complexity-performance tradeoff, the SFTF-DAE requires a careful initialization for maintaining numerical stability [36], making it less robust compared with the LMS-type sparse DAEs.

The complexity percentage of the PTU-DAEs to their full-tap counterparts are listed in Table V. At the same HT threshold 0.01, the complexity reduction is not as significant as that of the 16QAM case. However, a choice of 0.05 leads to considerable complexity reduction without affecting the performance much as already shown.

B. Second Experiment

The second experiment was conducted off the coastline of Sanya, Hainan, China, in August 2013. The ocean depth of the experiment area was about 80 m. The transmitter with single transducer was lowed to the depth of 15 m from a drifting boat. A vertical receive array with four hydrophones was lowed from an anchored boat. The top hydrophone in the array was about 13 m below the sea surface, and the spacing between adjacent hydrophones was 0.4 m. The relative

TABLE V
COMPLEXITY PERCENTAGE OF THE PTU-DAE TO THE FULL-TAP DAE
(2×4, QPSK)

DAE \ N_{dr}	2	4	6
PTU-NLMS(I)	99.62%	99.57%	99.51%
PTU-NLMS(II)	91.77%	90.45%	89.71%
PTU-IPNLMS(I)	91.64%	92.90%	93.73%
PTU-IPNLMS(II)	51.36%	52.45%	53.99%
PTU-SZA-NLMS(I)	94.22%	84.73%	78.53%
PTU-SZA-NLMS(II)	81.61%	69.91%	64.42%
PTU-SZA-IPNLMS(I)	86.84%	83.31%	80.95%
PTU-SZA-IPNLMS(II)	46.87%	46.41%	46.76%

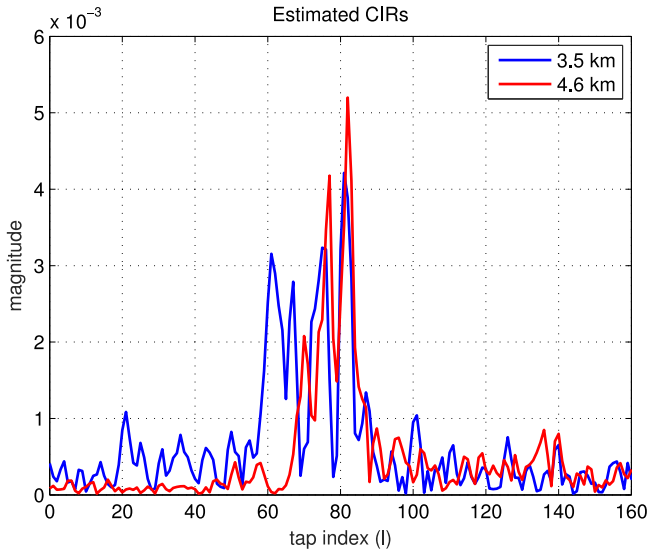

Fig. 5. Estimated CIRs for the second experiment.

TABLE VI
NEFB COMPARISON (1×4, QPSK, 288 BLOCKS IN TOTAL)

DAE \ N_{dr}	0	2	4	6
NLMS	88	232	258	269
PTU-NLMS	96	241	261	272
IPNLMS	209	260	272	276
PTU-IPNLMS	217	266	272	275
SZA-NLMS	93	237	258	267
PTU-SZA-NLMS	109	248	268	271
SZA-IPNLMS	205	261	273	275
PTU-SZA-IPNLMS	213	266	275	277
RLS	251	262	259	260
PTU-RLS	243	260	262	256

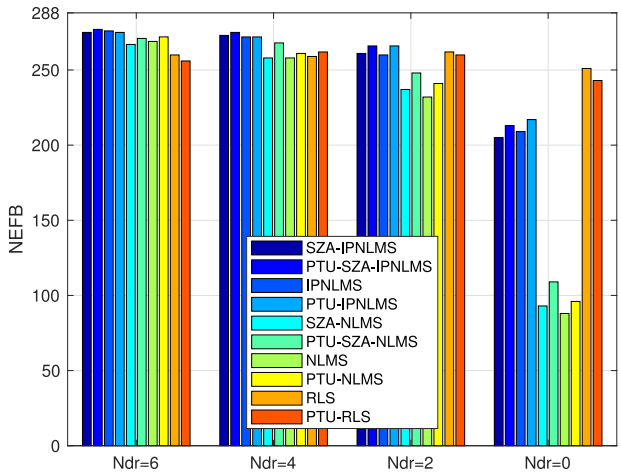

Fig. 6. Comparison of the NEFB (1×4, QPSK, 288 blocks in total).

TABLE VII
COMPLEXITY PERCENTAGE OF THE PTU-DAE TO THE FULL-TAP DAE
(1×4, QPSK)

DAE \ N_{dr}	0	2	4	6
PTU-NLMS	98.36%	98.33%	98.42%	98.55%
PTU-IPNLMS	22.26%	34.72%	45.19%	52.40%
PTU-SZA-NLMS	95.06%	73.74%	66.40%	63.35%
PTU-SZA-IPNLMS	19.22%	24.48%	28.17%	29.91%
PTU-RLS	98.47%	98.79%	98.94%	99.06%

speed between the transmitter and the receiver was about 1.6 kn. The communication distance was ~3.5 km (9 bursts collected) or ~4.6 km (15 bursts collected) and the average SNRs were 6.2 and 8.6 dB, respectively.

The carrier frequency was 8 kHz, the symbol period was 0.25 ms, and a rate-$(1/2)$ turbo channel code was adopted. Each transmission burst consisted of 12 blocks. Each block carried $K = 2136$ symbols, with the first $K_p = 200$ ones used for training purpose. The mean Doppler scale was estimated and compensated for each block, then the baseband signals were sampled at twice the symbol rate. The half-symbol-period equivalent multipath channels are shown by the examples in Fig. 5. A fractionally spaced LE was adopted. The LE parameters were: $K_1 = 81$, $K_2 = 80$, leading to an equalizer vector of size $L_w = 648$. The DAE parameters were the same as those in the first experiment, except that $\gamma_w = 2 \times 10^{-5}$ and $\gamma_w = 2 \times 10^{-6}$ were used for the SZA-NLMS-DAE and the SZA-IPNLMS-DAE, respectively. A forgetting factor $\lambda = 0.997$ was used for the RLS-DAE. To obtain PTU-DAEs, the HT threshold was set to 0.01.

The NEFB comparison based on 24 bursts (288 blocks) is shown in Table VI and Fig. 6. Though the performance difference among different DAEs is not as apparent as that of the first experiment, it is still seen the IPNLMS-DAE and the SZA-IPNLMS-DAE perform better than the SZA-NLMS-DAE and the NLMS-DAE. The performance gaps shrink as the DR repeat number increases. The PTU-DAEs almost consistently outperform their full-tap counterparts. The reason is that the LE with a large size of $L_w = 648$ faces a more serious noise enhancement issue compared with the smaller-size DFE employed in the first experiment. By discarding some trivial taps, the noise enhancement is alleviated and performance gain is achieved. The RLS-DAE again achieves a better performance than the LMS-type DAEs without DR and is not impacted by the DR much, as also shown in the first experiment. The PTU-RLS-DAE was also tested with comparable performance to the RLS-DAE.

The complexity percentage of the PTU-DAEs to their full-tap counterparts are listed in Table VII. The complexity reductions of the PTU-NLMS-DAE and PTU-RLS-DAE are negligible. In comparison,

the sparsity-aware DAEs enjoy considerable complexity savings. In particular, at $N_{\rm dr} = 6$, the PTU-SZA-IPNLMS-DAE achieves the most computation saving ($\sim$70%) and simultaneously the best performance.

VI. Conclusion

The sparse direct adaptive equalization for underwater acoustic communications was revisited and investigated in two unexplored aspects: First, a comprehensive comparison was made for DAEs designed with the PU principle and the ZA principle, respectively. It showed the PU-type sparse DAE is a better choice in terms of complexity, performance, and operability, and the reason is that an equalizer in general is not strictly sparse even the underlying channel is. The comparison also led to a sparse DAE design combining the PU and ZA mechanisms, which showed extra performance gain over existing sparse DAEs governed by single sparsity-promoting mechanism; second, the feasibility of PTU for sparse DAEs was verified in the sense that complexity reduction is achieved without sacrificing performance. The PTU was achieved via the HT method and with the same threshold, a sparse DAE actually enjoys more complexity reduction than a nonsparse one. In summary, this work demonstrated promising applications of sparse PTU-DAEs in single-carrier underwater acoustic communications. In the future work, focus will be given to the scenario where the sparse structure of a DAE is changing even within one transmission block. Advanced adaptive filtering algorithms and partial tap selection mechanisms will be investigated.

Appendix A

The first derivative of the l_1-norm of a complex vector $\mathbf{a}$ with respect to its conjugate $\mathbf{a}^*$ is computed as follows:

$$\begin{aligned}\frac{\partial \|\mathbf{a}\|_1}{\partial \mathbf{a}^*} &= \frac{\partial \sum_{p=1}^{P} |a_p|}{\partial \mathbf{a}^*} \\ &= \begin{bmatrix} \frac{\partial \sum_{p=1}^{P} |a_p|}{\partial a_1^*} \\ \frac{\partial \sum_{p=1}^{P} |a_p|}{\partial a_2^*} \\ \vdots \\ \frac{\partial \sum_{p=1}^{P} |a_p|}{\partial a_P^*} \end{bmatrix} = \begin{bmatrix} \frac{\partial \sum_{p=1}^{P} \sqrt{a_p a_p^*}}{\partial a_1^*} \\ \frac{\partial \sum_{p=1}^{P} \sqrt{a_p a_p^*}}{\partial a_2^*} \\ \vdots \\ \frac{\partial \sum_{p=1}^{P} \sqrt{a_p a_p^*}}{\partial a_P^*} \end{bmatrix} \\ &= \frac{1}{2} \begin{bmatrix} \frac{1}{\sqrt{a_1 a_1^*}} \frac{\partial a_1 a_1^*}{\partial a_1^*} \\ \frac{1}{\sqrt{a_2 a_2^*}} \frac{\partial a_2 a_2^*}{\partial a_2^*} \\ \vdots \\ \frac{1}{\sqrt{a_P a_P^*}} \frac{\partial a_P a_P^*}{\partial a_P^*} \end{bmatrix} = \frac{1}{2} \begin{bmatrix} \frac{a_1}{|a_1|} \\ \frac{a_2}{|a_2|} \\ \vdots \\ \frac{a_P}{|a_P|} \end{bmatrix}. \end{aligned} \tag{23}$$

Acknowledgment

J. Tao would like to thank Z. Qin for implementing the SFTF algorithm.

References

[1] M. Stojanovic, J. Catipovic, and J. Proakis, "Adaptive multichannel combining and equalization for underwater acoustic communications," *J. Acoust. Soc. Amer.*, vol. 94, no. 3, pp. 1621–1631, Sep. 1993.

[2] B. Geller, J. M. Broissier, and V. Capellano, "Equalizer for high data rate transmission in underwater communications," in *Proc. MTS/IEEE OCEANS Conf.*, 1994, pp. I/302–I/306.

[3] J. Tao, Y. R. Zheng, C. Xiao, and T. C. Yang, "Robust MIMO underwater acoustic communications using turbo block decision-feedback equalization," *IEEE J. Ocean. Eng.*, vol. 35, no. 4, pp. 948–960, Oct. 2010.

[4] L. Wang, J. Tao, and Y. R. Zheng, "Single-carrier frequency-domain turbo equalization without cyclic prefix or zero padding for underwater acoustic communications," *J. Acoust. Soc. Amer.*, vol. 132, no. 6, pp. 3809–3817, Dec. 2012.

[5] L. Wang, J. Tao, and Y. R. Zheng, "Low-complexity turbo detection for single-carrier low-density parity-check-coded multiple-input multiple-output underwater acoustic communications," *Wireless Commun. Mobile Comput.*, vol. 13, no. 4, pp. 439–450, Mar. 2013.

[6] S. Roy, T. M. Duman, V. McDonald, and J. G. Proakis, "High-rate communication for underwater acoustic channels using multiple transmitters and space-time coding: Receiver structures and experimental results," *IEEE J. Ocean. Eng.*, vol. 32, no. 3, pp. 663–688, Jul. 2007.

[7] A. Yellepeddi and J. C. Preisig, "Adaptive equalization in a turbo loop," *IEEE Trans. Wireless Commun.*, vol. 14, no. 9, pp. 5111–5122, Sep. 2015.

[8] C. Laot and R. L. Bidan, "Adaptive MMSE turbo equalization with high-order modulations and spatial diversity applied to underwater acoustic communications," in *Proc. Eur. Wireless*, Apr. 2011, pp. 1–6.

[9] J. Xi, S. Yan, L. Xu, and J. Tian, "Soft direct-adaptation based bidirectional turbo equalization for MIMO underwater acoustic communications," *China Commun.*, vol. 14, no. 7, pp. 1–12, Jul. 2017.

[10] F. Chen *et al.*, "Minimum symbol-error rate based adaptive decision feedback equalizer in underwater acoustic channels," *IEEE Access*, vol. 5, pp. 25147–25157, 2017.

[11] J. W. Choi, T. J. Riedl, K. Kim, A. C. Singer, and J. C. Preisig, "Adaptive linear turbo equalization over doubly selective channels," *IEEE J. Ocean. Eng.*, vol. 36, no. 4, pp. 473–489, Oct. 2011.

[12] Y. Wu and M. Zhu, "A low complexity multichannel adaptive turbo equalizer for a large delay spread sparse underwater acoustic channel," in *Proc. 4th Pacific Rim Underwater Acoust. Conf.*, Oct. 2013, pp. 49–55.

[13] Y. Wu, M. Zhu, and X. Li, "Sparse linear equalizers for turbo equalizations in underwater acoustic communication," in *Proc. MTS/IEEE OCEANS Conf.*, Washington, DC, USA, Oct. 2015, pp. 1–6.

[14] S. Haykin, *Adaptive Filter Theory*, 4th ed. Englewood Cliffs, NJ, USA: Prentice-Hall, 2001.

[15] S. Roy and J. J. Shynk, "Analysis of the data-reusing LMS algorithm," in *Proc. 32nd Midwest Symp. Circuits Syst.*, Aug. 1989, vol. 2, pp. 1127–1130.

[16] T. Aboulnasr and K. Mayyas, "Complexity reduction of the NLMS algorithm via selective coefficient update," *IEEE Trans. Signal Process.*, vol. 47, no. 5, pp. 1421–1424, May 1999.

[17] P. A. van Walree, "Channel sounding for acoustic communications: Techniques and shallow-water examples," Forsvarets Forskningsinstitutt, FFI-rapport 2011/00007, 2001.

[18] E. Vlachos, A. S. Lalos, and K. Berberidis, "Stochastic gradient pursuit for adaptive equalization of sparse multipath channels," *IEEE J. Emerg. Sel. Topics Circuits Syst.*, vol. 2, no. 3, pp. 413–423, Sep. 2012.

[19] Y. Huang, J. Benesty, and J. Chen, *Acoustic MIMO Signal Processing*, 1st ed. New York, NY, USA: Springer-Verlag, 2006.

[20] J. Benesty and S. L. Gay, "An improved PNLMS algorithm," in *Proc. IEEE Int. Conf. Acoust., Speech, Signal Process.*, 2002, vol. 2, pp. 1881–1884.

[21] O. Hoshuyama, R. A. Goubran, and A. Sugiyama, "A generalized proportionate variable step-size algorithm for fast changing acoustic environments," in *Proc. IEEE Int. Conf. Acoust., Speech, Signal Process. Conf.*, May 2004, vol. 4, pp. 161–164.

[22] Y. Chen, Y. Gu, and A. O. Hero, "Sparse LMS for system identification," in *Proc. Int. Conf. Acoust., Speech, Signal Process.*, 2009, pp. 3125–3128.

[23] Y. Gu, J. Jin, and S. Mei, "l0 norm constraint LMS algorithm for sparse system estimation," *IEEE Signal Process. Lett.*, vol. 16, no. 9, pp. 774–777, Sep. 2009.

[24] K. Pelekanakis and M. Chitre, "Comparison of sparse adaptive filters for underwater acoustic channel equalization/estimation," in *Proc. IEEE Int. Conf. Commun. Syst.*, Singapore, 2010, pp. 395–399.

[25] K. Pelekanakis and M. Chitre, "New sparse adaptive algorithms based on the natural gradient and the L_0-Norm," *IEEE J. Ocean. Eng.*, vol. 38, no. 2, pp. 323–332, Apr. 2013.

[26] Q. Meng, J. Huang, J. Han, C. He, and C. Ma, "An improved direct adaptive multichannel turbo equalization scheme for underwater communications," in *Proc. IEEE/MTS OCEANS Conf.*, 2012, pp. 1–5.

[27] W. Duan, J. Tao, and Y. R. Zheng, "Efficient adaptive turbo equalization for multiple-input-multiple-output underwater acoustic communications," *IEEE J. Ocean. Eng.*, vol. 43, no. 3, pp. 792–804, Jul. 2018.
[28] L. Liu, D. Sun, and Y. Zhang, "A family of sparse group Lasso RLS algorithms with adaptive regularization parameters for adaptive decision feedback equalizer in the underwater acoustic communication system," *Phys. Commun.*, vol. 23, pp. 114–124, Jun. 2017.
[29] Z. Qin, J. Tao, X. Wang, X. Luo, and X. Han, "Direct adaptive equalization based on fast sparse recursive least squares algorithms for multiple-input multiple-output underwater acoustic communications," *J. Acoust. Soc. Amer.*, vol. 145, no. 4, EL277–EL283, Apr. 2019.
[30] J. Tao, L. An, and Y. R. Zheng, "Enhanced adaptive equalization for MIMO underwater acoustic communications," in *Proc. MTS/IEEE OCEANS Conf.*, Anchorage, AK, USA, Sep. 2017, pp. 1–5.
[31] M. Stojanovic, J. Catipovic, and J. Proakis, "Phase-coherent digital communications for underwater acoustic channels," *IEEE J. Ocean. Eng.*, vol. 19, no. 1, pp. 100–111, Jan. 1994.
[32] S. Zhou and Z. Wang, *OFDM for Underwater Acoustic Communications*, Hoboken, NJ, USA: Wiley, Jun. 2014.
[33] J. G. Proakis and M. Salehi, *Digital Communication*, 5th ed. Upper Saddle River, NJ, USA: McGraw-Hill, 2008.
[34] J. Tao, "On low-complexity soft-input soft-output decision-feedback equalizers," *IEEE Commun. Lett.*, vol. 20, no. 9, pp. 1737–1740, Sep. 2016.
[35] D. T. M. Slock and T. Kailath, "Numerically stable fast transversal filters for recursive least squares adaptive filtering," *IEEE Trans. Signal Process.*, vol. 39, no. 1, pp. 92–114, Jan. 1991.
[36] L. Freitag, M. Johnson, and M. Stojanovic, "Efficient equalizer update algorithms for acoustic communication channels of varying complexity," in *Proc. MTS/IEEE OCEANS Conf.*, Halifax, NS, Canada, 1997, vol. 1, pp. 580–585.
[37] J. Tao, "On low-complexity soft-input soft-output linear equalizers," *IEEE Wireless Commun. Lett.*, vol. 5, no. 2, pp. 132–135, Apr. 2016.

Jun Tao (S'10–M'10) received the B.S. and M.S. degrees in electrical engineering from the Department of Radio Engineering, Southeast University, Nanjing, China, in 2001 and 2004, respectively, and the Ph.D. degree in electrical engineering from the University of Missouri, Columbia, MO, USA, in 2010.

From 2004 to 2006, he was a System Design Engineer with Realsil Microelectronics, Inc. (a subsidiary of Realtek), Suzhou, China. From 2011 to 2015, he was a Senior System Engineer with Qualcomm, Inc., Boulder, CO, USA, working on the baseband algorithm and architecture design for the UMTS/LTE modem. Since April 2016, he has been with the School of Information Science and Engineering, Southeast University, Nanjing, as a Full Professor. His research interests lie in the general areas of wireless cellular communications, underwater acoustic communications, and localization and tracking, including channel modeling and estimation, turbo equalization, adaptive filtering, Bayesian inference, and machine learning.

Yanbo Wu received the B.S. and Ph.D. degrees in electronic engineering from the Beijing Institute of Technology, Beijing, China, in 2003 and 2008, respectively.

Since 2008, he has been with the Institute of Acoustics, Chinese Academy of Sciences, Beijing, where he is currently a Professor with the Ocean Acoustic Technology Center. His research interests include turbo equalization, channel codes, and underwater acoustic communications.

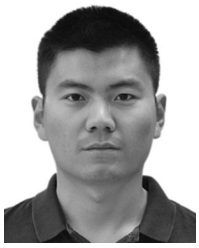

Xiao Han received the B.S., M.S., and Ph.D. degrees in underwater acoustic engineering from Harbin Engineering University, Harbin, China, in 2011, 2014, and 2016, respectively.

He is currently an Assistant Professor with the College of Underwater Acoustic Engineering, Harbin Engineering University. He is also a member of Acoustical Society of China. He has been a Visiting Scholar with Acoustic Research Laboratory, National University of Singapore, since April 2019. He has authored or coauthored numerous research articles in related journals and international conference proceedings. He is the holder of 13 patents. His research interests include underwater acoustic communication and underwater array signal processing.

Konstantinos Pelekanakis (S'06–M'09–SM'17) received the Diploma degree from the Department of Electronic and Computer Engineering, Technical University of Crete, Crete, Greece, in 2001, and the M.Sc. and Ph.D. degrees in mechanical and ocean engineering from the Massachusetts Institute of Technology (MIT), Cambridge, MA, USA, in 2004 and 2009, respectively.

From 2009 to 2015, he worked with the Acoustic Research Laboratory, National University of Singapore as a Research Fellow. From 2011 to 2014, he also worked as a Lecturer for the Master of Defence Technology and Systems Programme, Temasek Defence Systems Institute, Singapore. He is currently a Senior Scientist with the NATO Science and Technology Organization, Centre for Maritime Research and Experimentation, La Spezia, Italy. In 2018, he was awarded the NATO Scientific Achievement Award for contributing in the development of JANUS, the first digital underwater communications standard. His main research area is statistical signal processing for underwater acoustic communications.

Dr. Pelekanakis has served as the Secretary and Vice Chairman for the IEEE OES Singapore chapter in 2013 and 2014, respectively. He has served in the organizing committee for the IEEE UComms 2016 and 2018. He also serves as an Associate Editor for the IEEE JOURNAL OF OCEANIC ENGINEERING. He has been awarded with MIT Presidential Fellowship in 2001.